Quasi-static growth of bubbles in a gelatin gel under dissolved-gas supersaturation

Keita Ando[1,a)] and Eriko Shirota[1]

AFFILIATION
[1]Department of Mechanical Engineering, Keio Univeristy, 3-14-1 Hiyoshi, Kohoku-ku, Yokohama 223-8522, Japan
[a)]Electronic mail: kando@mech.keio.ac.jp

ABSTRACT

We theoretically and experimentally study quasi-static growth of bubbles in a gelatin gel under dissolved-gas supersaturation in order to examine the role of the gel elasticity in the mass-diffusion-driven process. First, we model the diffusion-driven bubble growth with the classical Epstein-Plesset approach for quasi-static bubble growth, accounting for elasticity of the medium surrounding bubbles. Next, we devise an experimental technique to visualize bubble growth in an air-supersaturated gel of different gelatin concentrations and obtain the growth rate of the bubble. We show, from comparisons between the theory and experiments, that the bubble growth is hindered by the gel elasticity.

Bubbles can nucleate and grow under supersaturation of gases dissolved in liquids and viscoelastic materials: carbonated beverages, magmatic melts, food, and tissues.[1,2,3,4] One of the representative examples is decompression sickness caused by the formation of gas bubbles in human blood and tissues; bubbles nucleate under rapid decompression in divers' body and then grow by transfer of dissolved gases, giving rise to blood-flow interruption.[5] Since the mass-diffusion-driven growth of bubbles is very gradual, effects of the bubble interface advection are often negligible. The Epstein-Plesset (EP) theory models the quasi-static growth of single spherical bubbles driven by mass diffusion in liquids, which is derived from the Young-Laplace equation and the diffusion equation with spherical symmetry.[6] The EP theory for bubbles in liquids has been validated through comparisons to experiments.[7] However, little is theoretically and experimentally studied regarding the effect of elasticity of the medium surrounding bubbles on their thermodynamic stability with regard to mass diffusion. In this letter, we theoretically and experimentally study the diffusion-driven growth of single bubbles in a gelatin gel supersaturated with dissolved gas in order to examine the role of elasticity. In what follows, we present theoretical and experimental methods for studying bubble growth in gas-supersaturated gels, which allows for quantification of elasticity effects on the bubble growth.

First, we revisit the EP theory[6] that describes bubble growth in liquids under dissolved gas supersaturation and extend it to the case of bubbles in elastic media as depicted in Fig. 1. The target of the original EP theory is the quasi-static growth of a single bubble with no translation in gas-supersaturated liquids. Since mass-diffusion-driven bubble growth is very gradual in many cases (e.g., air-water systems), the liquid-phase advection by the bubble

growth is negligible and the bubble behaves isothermally. Under this situation, the evolution of bubble radius R in mechanical equilibrium is determined from Fick's mass diffusion equation (with spherical symmetry)[8]

$$\frac{dR}{dt} = D\left(\frac{1}{R} + \frac{1}{\sqrt{\pi Dt}}\right)\frac{c_\infty - c_{s0}\left(1+\frac{2\sigma}{Rp_\infty}\right)}{\rho_{g0}\left(1+\frac{4\sigma}{3Rp_\infty}\right)}, \tag{1}$$

where D is the binary diffusion constant, c_∞ is the mass concentration of gas dissolved in liquids (away from the bubble), c_{s0} and ρ_{s0} are the saturated gas concentration (determined from Henry's law) and the gas density inside the bubble, respectively, at one atmosphere p_∞, and σ is the surface tension. The thickness of the concentration boundary layer developing from the bubble interface is given by $\sqrt{\pi Dt}$ and set to 0 initially at bubble nucleation (t = 0). In the original theory, the gas pressure p_g inside the bubble in mechanical equilibrium is given by the Young-Laplace equation ($p_g = p_\infty + (2\sigma/R)$). However, when it comes to considering bubbles in elastic media, there is a need to account for elasticity in computing the gas pressure. In the case of linear elastic solids, it is computed by[9,10]

$$p_g = p_\infty + \frac{2\sigma}{R} + \frac{4G}{3}\left[1 - \left(\frac{R_{\mathrm{sf}}}{R}\right)^3\right], \tag{2}$$

where G is the rigidity (or the shear modulus) and R_{sf} represents the equilibrium radius at which the surrounding medium is strain-free. In this case, the original EP Eq. (1) becomes

$$\frac{dR}{dt} = D\left(\frac{1}{R} + \frac{1}{\sqrt{\pi Dt}}\right)\frac{c_\infty - c_{s0}\left(1+\frac{2\sigma^*}{Rp_\infty}\right)}{\rho_{g0}\left(1+\frac{4\sigma}{3Rp_\infty}+\frac{4G}{3p_\infty}\right)}, \tag{3}$$

where the effective surface tension σ^* is defined by

$$\sigma^* = \sigma + \frac{2GR}{3}\left[1 - \left(\frac{R_{\mathrm{sf}}}{R}\right)^3\right]. \tag{4}$$

Note that the effective value σ^* under bubble growth beyond the strain-free state (i.e., $R > R_{\mathrm{sf}}$) gets larger than the physical value σ. This is caused by elasticity of the surrounding medium that works as restoring force.

Next, we present an experimental approach to see effects of elasticity on the diffusion-driven bubble growth. A gelatin gel is used as an elastic medium; the gel elasticity is tuned by changing the mass concentration (3, 5, and 7 wt. %) of gelatin extracted from porcine skin (G2500, Type-A, Sigma-Aldrich). Gelatin and water are mixed and heated to create gelatin solutions. The solutions are poured into an acrylic container (lateral dimensions: 34 mm × 34 mm, height: 15 mm) whose bottom is sealed with a wrapping film. Then, the solutions are solidified in a fridge (approximately at 6°C) for 24 hours. After the gelatin gel phantom is taken out of the fridge, it is soaked in a water tank and eventually reaches thermal equilibrium at the room temperature (approximately 23°C). Since mass diffusion of dissolved air is much slower, the gel just after the thermal equilibrium is reached is under the dissolved gas supersaturation.[9,10] We make an estimate of the gas supersaturation $\zeta = (c_\infty - c_{s0})/c_{s0}$ at a bubble nucleation spot based on the analytical solution[12] of one-dimensional diffusion equation with uniform diffusivity D and initially uniform supersaturation ζ_∞ (determined from Henry's constants at 6°C and 23°C); as boundary conditions, the saturation condition (i.e., Henry's law) at one atmosphere p_∞ is imposed at the gel surface open to the atmosphere and the insulated

condition is imposed at the film-sealed bottom. Since the value of D for air-gel systems is unavailable from literature, we use the value for air-water systems as a rough estimate. We consider the case for which the gas supersaturation is slight ($\zeta \approx 0.1$). The surface tension[13] of the gelatin gel, which is used in solving the extended EP model equation, is documented in Table 1.

With this gel sample, we perform visualization of bubble growth under the gas supersaturation. The optical setup is depicted in Fig. 2. Bubble nucleation is triggered by focusing an infrared laser pulse (1064 nm, 6 ns, 3.7±0.1 mJ) through an objective lens (40×, NA = 0.6) into the gas-supersaturated gel. The subsequent growth of the nucleated bubble driven by influx of dissolved air is captured through a CCD camera (pixelfly, pco.) at 1 frame every 5 seconds through 40× magnification. The bubble's sphericity is defined by $4\pi(\text{Area})/(\text{Perimeter})^2$ and calculated from the captured image (as will be presented in Fig. 3) with MATLAB image processing. It turns out to range from 0.98 to 1.02, meaning that the bubbles keep being fairly spherical. The area-equivalent radius R can thus be used for comparisons to the EP theory (Eq. (3)) whose target is spherical bubbles. The container size is large enough, in comparison to the thickness of the concentration boundary layer in our observation span, to guarantee the spherical symmetry of the problem as depicted in Fig. 1. Moreover, it is important to note the gel rigidity measurement used for the gel sample. Ideally, the gel sample (without the laser focusing) may have uniform rigidity. However, the laser-induced phenomena (including plasma formation, shockwave emission, and inertial bubble growth) will give rise to structural damage in the gel.[11] It is likely that rigidity of the gel in the vicinity of the laser-induced gas bubble nuclei is reduced, necessitating local measurement of the gel rigidity. According to Ref. 14, we perform ultrasound-based rigidity measurement in which 1-MHz ultrasound is irradiated toward the bubble in the gel and the bubble translation under the acoustic radiation force is recorded by a camera; the rigidity of the gel in the vicinity of the bubble can be calculated, together with a linear elastic model, from the measured translation. The measured rigidity is documented in Table 1.

Here, we present the experimental results and discuss them with the extended EP theory. Figure 3 shows sequential images of a bubble in the gel of three different gelatin concentrations; these bubbles are under similar gas supersaturation ($\zeta \approx 0.1$); the corresponding movies (up to 1000 s after the bubble nucleation) with higher image resolution are available online as supplementary material. The bubble initially shows shrinkage (between the first and second frames in Fig. 3) due to the gel elasticity and then gradual growth, driven by mass diffusion, after minimum radius $R_{\min}$ is reached. The area-equivalent radius is calculated from these images and plotted in Fig. 4 as a function of time (measured from the laser focusing). The characteristic radii (R_0, $R_{\min}$) where R_0 represents the radius of the nucleated bubble captured in the initial frame of Fig. 3 are reported in Table 2. We see that the growth rate is hindered by increasing the gelatin concentration (or increasing the gel elasticity). The observed growth ($t > t_{\min}$) is compared to the extended EP theory (Eq. (3)); see Fig. 5. In plotting the model prediction, the unknown value of R_{sf} is treated as a fitting parameter. The computation of Eq. (3) starts from $t = t_{\min}$ when the minimum radius $R_{\min}$ is reached. For simplicity, the

boundary layer thickness δ_c is set to 0 as the initial condition (at $t = t_{min}$), but the choice of the initial thickness does not have an impact on the overall computation. It follows from Fig. 5 that the extended EP theory can well reproduce the bubble growth, with the fitted value of R_{sf} (see Table 2). For reference, the computation for water (with no rigidity $G = 0$) is plotted in this figure; the growth rate in the absence of rigidity-produced restoring force shows faster than that with rigidity. This suggests that accounting for elasticity in the EP theory is essential in order to accurately predict the diffusion-driven growth of bubbles in gas-supersaturated gels. We can also say, in this example, that the gelatin gel behaves as linear elastic solids, at least up to $R/R_{min} \approx 2$. Finally, we note that the pre-strain ($R_{sf} < R_{min}$) in the gel of the highest gelatin concentration (7 wt. %) is emphasized, while it is negligible ($R_{sf} \approx R_{min}$) in the gel of the lower concentrations. Hence, there is a need to incorporate such pre-strain effect in modeling the diffusion-driven growth of laser-induced bubbles in gels of high gelatin concentrations.

In summary, we demonstrated that the gel elasticity hinders the diffusion-driven growth of laser-induced bubbles in the gas-supersaturated gel and its effect can be incorporated in the EP theory. As future work, one may consider further extensions to the theory such as nonlinear elasticity[15,16,17] and cavitation-induced gel structure damage.[18]

SUPPLEMENTARY MATERIAL

See supplementary material for higher-resolution movies (up to 1000 s after the bubble nucleation) corresponding to Fig. 3. The movie files (named movie1, movie2, and movie3) are for the case of gelatin concentration at 3, 5, and 7 wt. %, respectively.

ACKNOWLEDGEMENTS

This study was supported by JSPS KAKENHI Grant Number 17H04905. The authors would like to thank Dr. Tatsuya Yamashita for his support in the data analysis.

REFERENCES

[1]M. Robinson, A.C. Fowler, A.J. Alexander, and S.B.G. O'Brien, Waves in Guinness. *Phys. Fluids* **20**, 067101 (2008).
[2]G.Y. Gor and A.E. Kuchma, Dynamics of gas bubble growth in a supersaturated solution with Sievert's solubility law. *J. Chem. Phys.* **131**, 034507, 1-7 (2009).
[3]A.A. Chernov, V.K. Kedrinsky, and A.A. Pil'nik, Kinetics of gas bubble nucleation and growth in magmatic melt at its rapid decompression. *Phys. Fluids* **26**, 116602 (2014).
[4]P. Shah, G.M. Champbel, S.L. Mckee, and C.D. Rielly, Proving of bread dough: modeling the growth of individual bubbles. *Trans. Inst. Chem. Eng.* **76**, 73-39 (1998).
[5]J.M. Solano-Altamirano and S. Goldman, The lifetimes of small arterial gas emboli, and their possible connection to inner ear decompression sickness. *Math. Biosci.* **252**, 27-35 (2014).
[6]P.S. Epstein and M.S. Plesset, On the stability of gas bubbles in liquid-gas solutions. *J. Chem. Phys*. **18**, 1505-1509 (1950).
[7]T. Yamashita and K. Ando, Aeration of water with oxygen microbubbles and its purging effect. *J. Fluid Mech.* **825**, 16-28 (2017).
[8]C.E. Brennen, *Cavitation and Bubble Dynamics* (Cambridge University Press, 2013).

[9]C. Hua and E. Johnsen, Nonlinear oscillations following the Rayleigh collapse of a gas bubble in a linear viscoelstic (tissue-like) medium. *Phys. Fluids* **25**, 083101 (2013).
[10]F. Hamaguchi and K. Ando, Linear oscillation of gas bubbles in a viscoelastic material under ultrasound irradiation. *Phys. Fluids* **27**, 113103 (2015).
[11]R. Oguri and K. Ando, Cavitation bubble nucleation induced by shock-bubble interaction in a gelatin gel. *Phys. Fluids* **30**, 051904 (2018).
[12]R. Haberman, *Applied Partial Differential Equations* (Pearson, 2013).
[13]J.H. Johnston and G.T. Pread, The surface tension of gelatin solutions. *Biochem. J.* **19**, 281-289 (1925).
[14]E. Shirota and K. Ando, Estimation of mechanical properties of gelatin using a microbubble under acoustic radiation force. *J. Phys.: Conf. Ser.* **656**, 012001 (2015).
[15]R. Gaudron, M.T. Warnez, and E. Johnsen, Bubble dynamics in a viscoelastic medium with nonlinear elasticity, *J. Fluid Mech.* **766**, 54-75 (2015).
[16]M.T. Warnez and E. Johnsen, Numerical modeling of bubble dynamics in viscoelastic media with relaxation, *Phys. Fluids* **27**, 063103 (2015).
[17]C.T. Wilson, T.L. Hall, E. Johnsen, L. Mancia, M. Rodriguez, J.E. Lundt, T. Colonius, D.L. Henann, C. Franck, Z. Xu, and J.R. Sukovich, A comparative study of the dynamics of laser and acoustically generated bubbles in viscoelastic media, *Phys. Rev. E* **99**, 043103 (2019).
[18]P. Movahed, W. Kreider, A.D. Maxwell, S.B. Hutchens, and J.B. Freund, Cavitation-induced damage of soft materials by focused ultrasound bursts: A fracture-based dynamics model. *J. Acoust. Soc. Am.* **140**, 1374-1386 (2016).

FIGURES AND TABLES

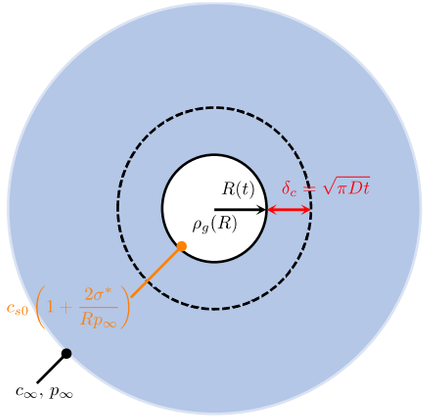

FIG. 1 Schematic of a growing bubble in an elastic medium supersaturated with dissolved gas ($c_\infty > c_{s0}[(1 + 2\sigma^*/(Rp_\infty)]$). The concentration boundary layer of thickness δ_c develops radially from the bubble interface.

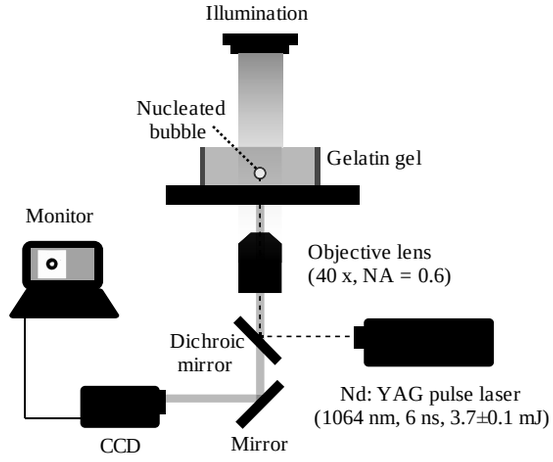

FIG. 2 Experimental setup for triggering bubble nucleation in a gas-supersaturated gel and observing the subsequent growth of the bubble.

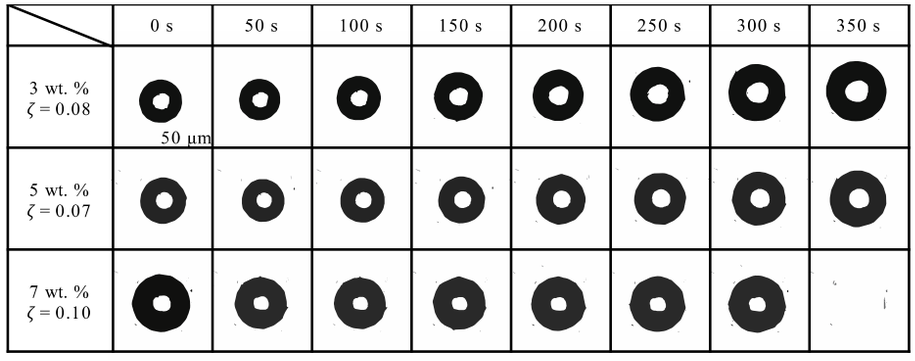

FIG. 3 Sequential images of a bubble in the gel of different gelatin concentration under dissolved-air supersaturation ($\zeta > 0$). Time is measured from the initial frame of the recording just after the laser focusing. The corresponding movies (up to 1000 s after the bubble nucleation) with higher resolution are available online as supplementary material.

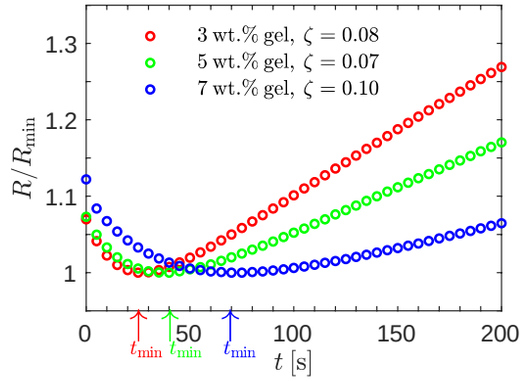

FIG. 4 Evolution of the area-equivalent radius of the bubble in the gel, under dissolved gas supersaturation ($\zeta > 0$), which is obtained from postprocessing the images in Fig. 3. The radius is normalized by its minimum value encountered at time t_{min} (denoted by vertical arrows).

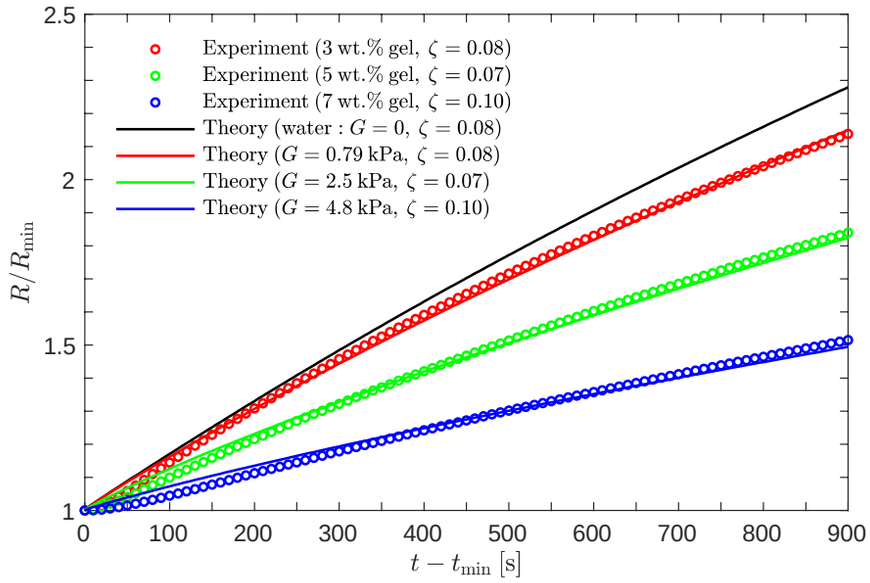

FIG. 5 Comparison in the evolution of the diffusion-driven bubble growth ($t > t_{min}$) between the experiments (symbols) and the extended EP theory (lines). In plotting the model prediction, the strain-free radius R_{sf} is treated as a fitting parameter; see its value in Table 2.

TABLE 1 Surface tension σ and rigidity G of the gel with varying gelatin concentration at the room temperature (23°C).

Gel. cont. [wt. %]	σ [N/m]	G [kPa]
0	0.072	0
3	0.064	0.79
5	0.063	2.5
7	0.062	4.8

TABLE 2 Characteristic radii (R_0, R_{min}, R_{sf}) of the bubble as a function of gelatin concentration where R_0 represents the radius of the nucleated bubble captured in the initial frame of Fig. 3.

Gel. cont. [wt. %]	R_0 [μm]	R_{min}/R_0	R_{sf}/R_0
3	31.4	0.93	0.93
5	33.2	0.93	0.91
7	44.2	0.89	0.58

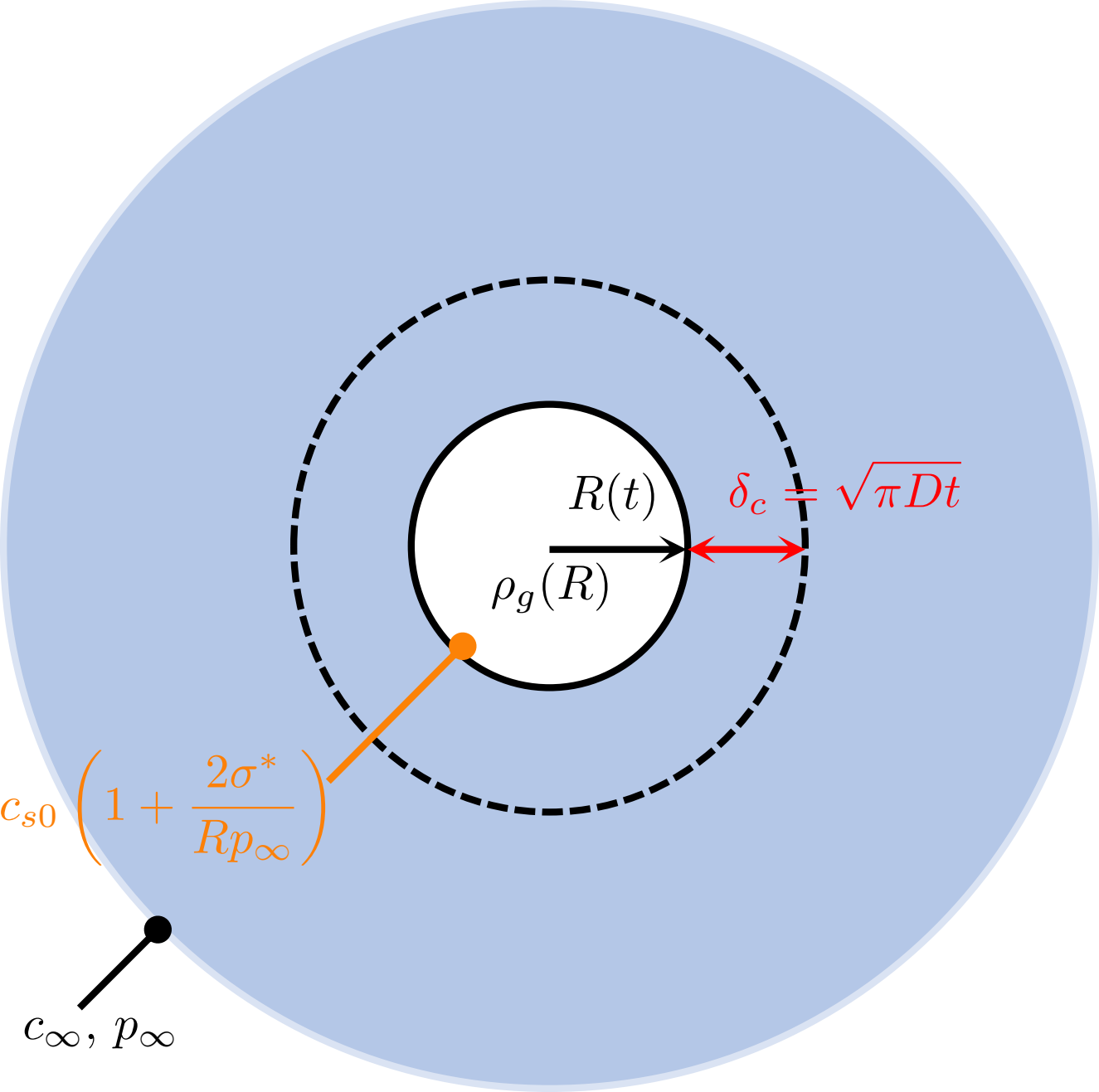
$R(t)$
$\delta_c = \sqrt{\pi D t}$
$\rho_g(R)$
$c_{s0}\left(1 + \frac{2\sigma^*}{Rp_\infty}\right)$
$c_\infty,\ p_\infty$

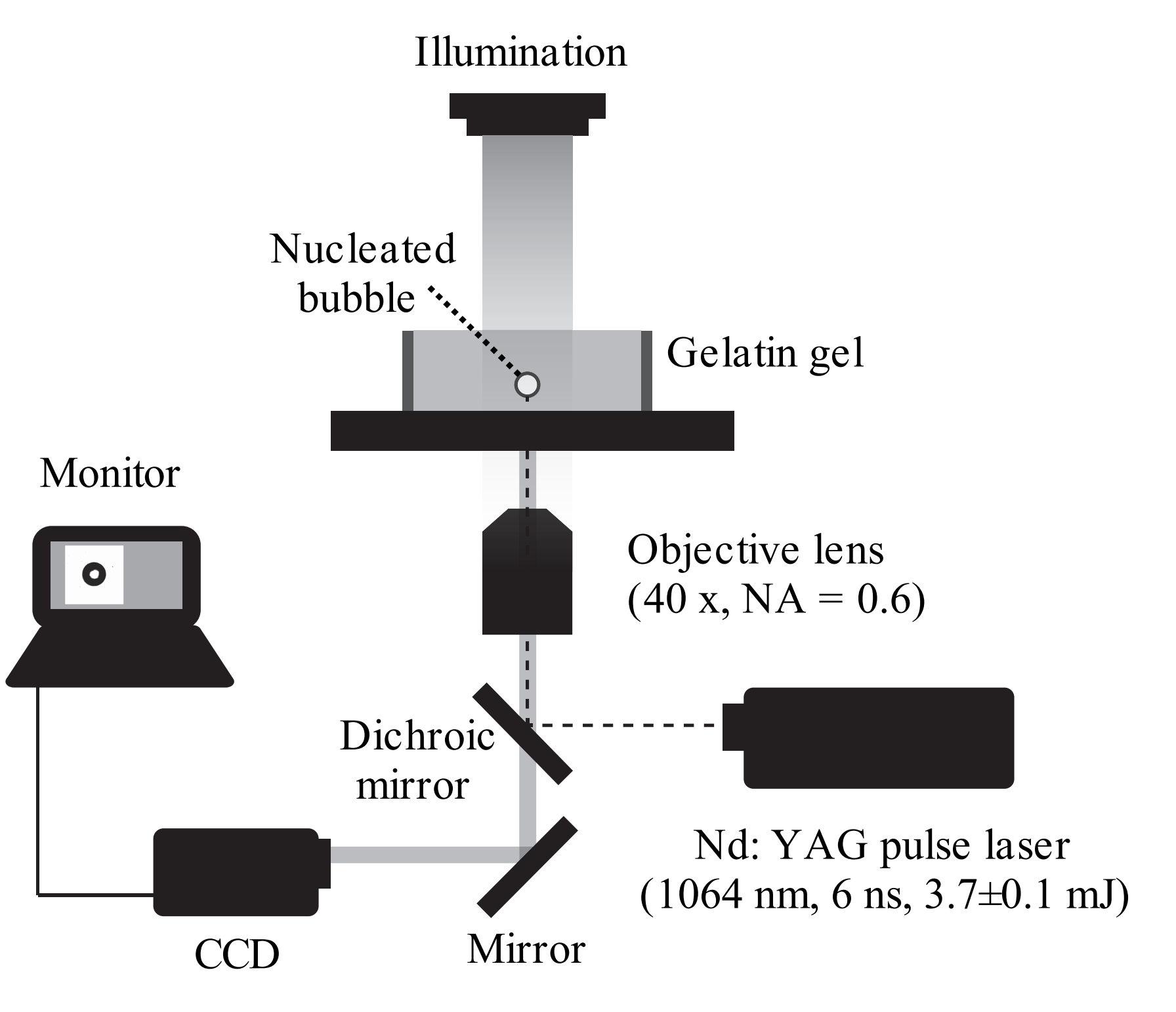
Illumination
Nucleated bubble
Gelatin gel
Monitor
Objective lens (40 x, NA = 0.6)
Dichroic mirror
Nd: YAG pulse laser (1064 nm, 6 ns, 3.7±0.1 mJ)
CCD
Mirror

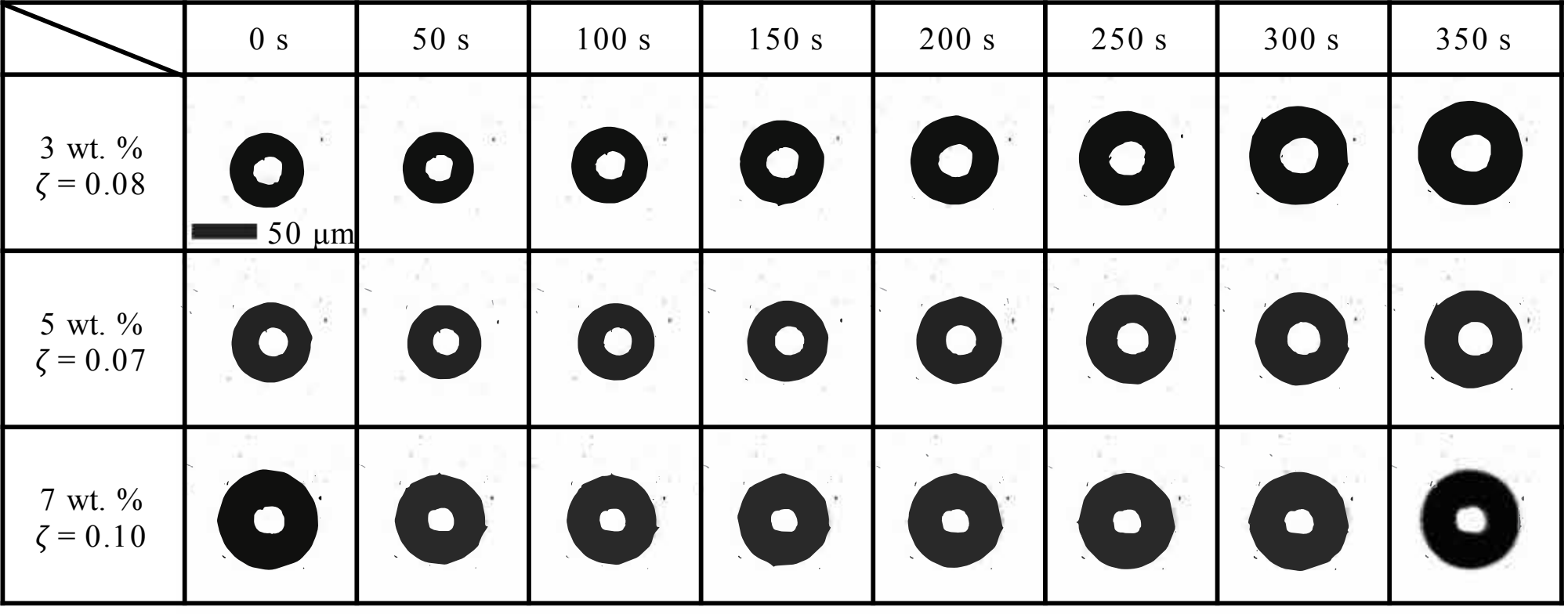
0 s
50 s
100 s
150 s
200 s
250 s
300 s
350 s
3 wt. %
ζ = 0.08
50 μm
5 wt. %
ζ = 0.07
7 wt. %
ζ = 0.10

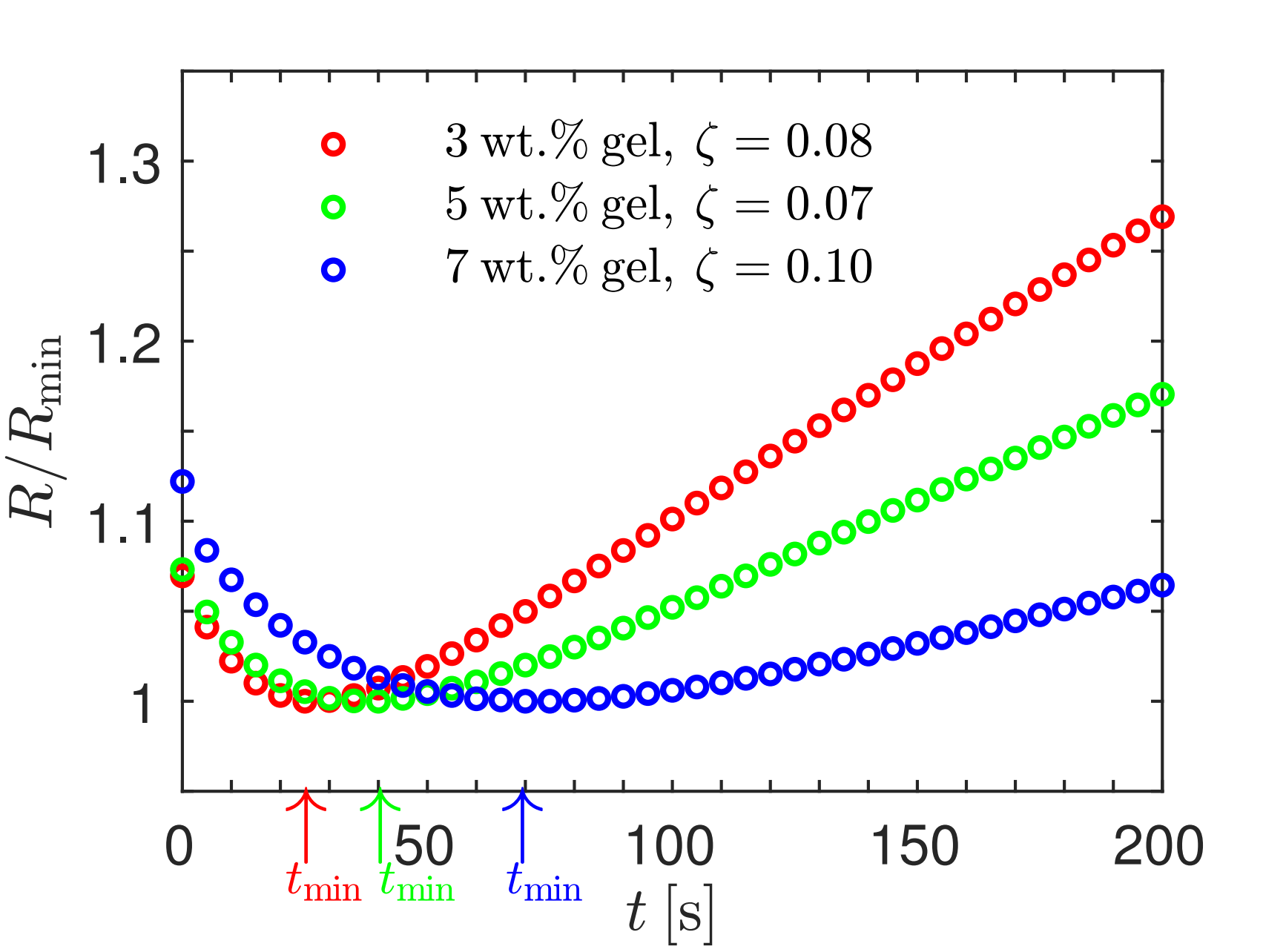
3 wt.% gel, $\zeta = 0.08$
5 wt.% gel, $\zeta = 0.07$
7 wt.% gel, $\zeta = 0.10$
R/R_{min}
1.3
1.2
1.1
1
0
50
100
150
200
t_{min}
t_{min}
t_{min}
t [s]

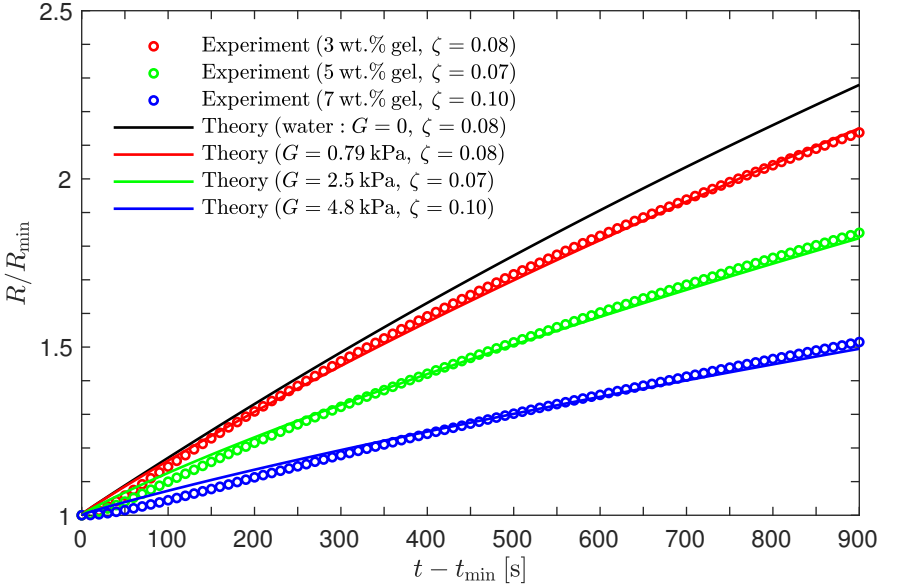
Experiment (3 wt.% gel, $\zeta = 0.08$)
Experiment (5 wt.% gel, $\zeta = 0.07$)
Experiment (7 wt.% gel, $\zeta = 0.10$)
Theory (water : $G = 0$, $\zeta = 0.08$)
Theory ($G = 0.79$ kPa, $\zeta = 0.08$)
Theory ($G = 2.5$ kPa, $\zeta = 0.07$)
Theory ($G = 4.8$ kPa, $\zeta = 0.10$)
$R/R_{\min}$
$t - t_{\min}$ [s]
2.5
2
1.5
1
0
100
200
300
400
500
600
700
800
900